A Novel X-Band, Circularly Polarized Feed For The I-30 Radar Antenna System

F. A. Lauriente and W. E. Hord
Microwave Applications Group, Santa Maria, California

This paper describes a novel application of septum polarizers in the realization of a feed system for I-30 Radar Antenna System. The I-30 antenna is an electronically steerable phased array employing nonreciprocal, curcularly polarized ferrite phase shifters in a transmission (bootlace) lens arrangement with a space feed. The feed is required to provide monopulse operation with either sense of circular polarization on receive, as well as the duplexing function between the transmit and receive modes of operation with the sense of the transmit polarization being opposite to that on receive.

The feed uses a square multi-mode pyramidal horn. Flare angle changes are utilized for the generation of higher order waveguide modes to obtain equal E- and H-plane primary patterns for efficient illumination of the phased lens commensurate with low spillover loss. A cruciform arrangement of four stepped septum polarizers excites the throat of the horn. The transmit ports of the polarizers are combined with magic tees to form a transmit sum port, and the receive ports are combined in an off-the-shelf monopulse comparator which forms the receive sum port and two orthogonal difference ports.

I. Introduction

The I-30 radar system is a “sophisticated threat” radar simulator. The radar consists of a two-axis electronically scanned phased array antenna, a coherent high-power transmitter, superheterodyne 3-channel receiver and digital signal processor all operating under control of a Concurrent model 7500 radar control computer. The radar features extremely fast beam scan rates, monopulse tracking, real-time simulation capabilities and high throughput digital signal processing.

The I-30 antenna is a transmission (bootlace) lens illuminated by a space feed. Nonreciprocal ferrite phase shifters operating in a circularly polarized mode are contained between an aperture plate and a feed plate. Radiating elements are formed when dielectric transformers on each end of the ferrite phase shifters are inserted into circular cavities bored in the feed and aperture plates. Since the single-bounce target return is desired, the received circular polarization is opposite the transmitted circular polarization and commutation of the phase shifters is not required. Accordingly, the phase shifters are switched at the beam scan rate rather than at twice the radar pulse repetition frequency which minimizes power supply requirements.

II. Functional Description Of The I-30 Antenna System

The I-30 antenna consists of a transmission lens, a three-channel monopulse feed, an r-f switch for selection of either two or three-channel monopulse operation, a beam steering computer, the power supplies necessary to power the system and a structure for mounting and/or support of the various subsystems. A block diagram is given in Figure 2-1, and the antenna specifications are given in Table 2-1.

The antenna is designed to radiate either sense of circular polarization and to receive the opposite sense circular polarization. All subsystems are pressurized to prevent penetration of the system by foreign matter. Built-in-test is incorporated into the design, so that the beam steering computer acts as a diagnostic/protective subsystem in addition to carrying out its normal control function. Sidelobe blanking antennas—one for each sense circular polarization—are incorporated into the radiating aperture. The final configuration is shown in Figure 2-2, and a list of features is given in Table 2-2.

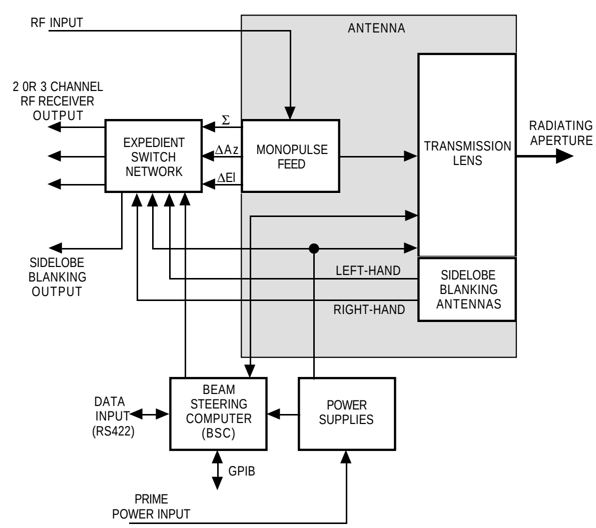

Fig. 2-1 System Block Diagram

Table 2-1
I-30 Antenna Specifications

Frequency Range	8.3 GHz - 8.9 GHz
Instantaneous Bandwidth	50 MHz
Polarization	Circular
Azimuth Scan	±20 degrees
Elevation Scan	±22.5 degrees
VSWR	1.50:1 Max.
Gain (Broadside)	36 dB Max.
Peak Power	100kW
Average Power	8kW
Beamwidth	1.9 Degrees AZ and EL
Beam Pointing Accuracy	0.25 Milliradians Max.
Beam Resolution	0.25 Milliradians
Beam Broadening	0.3 Degrees Max.
Peak Sidelobe Level	-25 dB Max.
Beam Switching Time	100 Microseconds Max.
Load Time	500 Microseconds Max.
Operating Temperature	-15 to 46 Degrees C

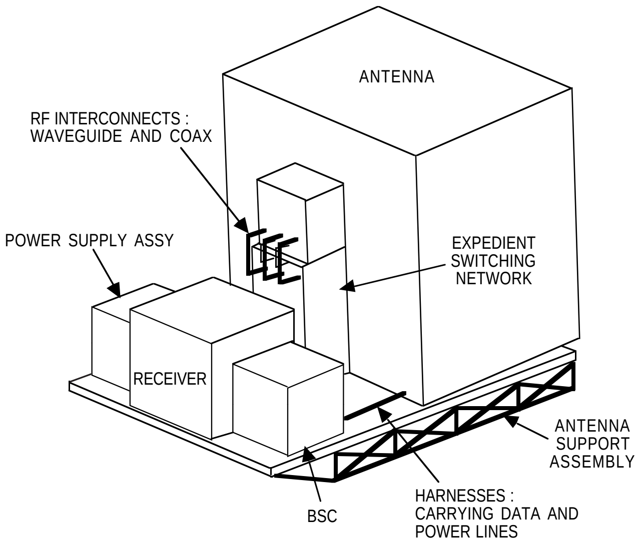

Fig. 2-2 I-30 Antenna System Configuration

Table 2-2
I-30 Antenna Features

- 2101 Radiating Elements Located on an Isosceles Triangle Grid
- 50 Inch Circular Aperture
- 50 Inch Focal Length
- Circular Polarization
  - Transmit Right Hand, Receive Left-Hand
  - Or Transmit Left-Hand, Receive Right-Hand
- 3-Channel Monopulse Comparator
- Latching Ferrite Phase Shifters
- Sidelobe Blanking Antennas
- Built-in-Test
- Pressurized Assembly
- Heat Pipes for Passive Array Cooling

THE OCCURRENCE OF ANY OF THE CONDITIONS WILL CAUSE THE BSC TO SET THE FAULT LINE AND DISABLE ANTENNA SWITCHING

- Loss of 208 Volt A-C Power Source
- Loss of 5 Volt Power Supply
- Loss of 15 Volt Power Supply
- Loss of ±12 Volt Power Supply
- Array Overtemperature Condition
- BSC Overtemperature Condition
- Self Test Failure

MONITORED STATUS INCLUDE THE FOLLOWING

- Power Supply Status
- Cooling Fan Status
- Polarization Status
- I/O Status
- Bit Status
- Self Test Status

Antenna efficiency factors are shown in Table 2-3 leading to a predicted gain of 37 dB.

Table 2-3
Efficiency Factors
D = 50.0 IN., N = 2101

EFFICIENCY FACTOR (dB)	*FREQUENCY (GHz)*		
Parameter	8.30	8.60	8.90
Illumination Taper	-0.46	-0.52	-0.59
Spillover	-0.51	-0.44	-0.38
Phase Errors (σ = 15°)	-0.29	-0.29	-0.29
Amplitude Errors (σ = 0.06)	-0.02	-0.02	-0.02
Cross-Polarization	-0.22	-0.16	-0.22
Diffraction	-0.09	-0.11	-0.20
Phase Shifter Loss (dB)	-1.3	-1.2	-1.2
Phase Shifter Quantization (7-bit)	-0.0	-0.0	-0.0
Feed Loss (dB)	-0.30	-0.30	-0.30
Mismatch Loss (1.75:1)	-0.34	-0.34	-0.34
Total Efficiency (dB)	-3.53	-3.38	-3.54
Maximum Aperture Gain (dB)	40.61	40.90	41.17
Net Antenna Gain Boresight (dB)	37.08	37.52	37.63
3 dB Beam Width Boresight (Degrees)	1.93	1.88	1.84

The phase characteristics of the nonreciprocal ferrite phase shifters are shown in Figure 2-3. Note the phase characteristics are symmetrical about the vertical axis. If the phase required of a particular element for antenna collimation is $ø_1$, the diagram suggests the antenna will be collimated for right-hand circularly polarized waves propagating in the +z direction and left-hand circularly polarized waves propagating in the -z direction. This implies that the antenna is self-duplexing if a means is provided at the feed to separate orthogonal senses of circular polarization.

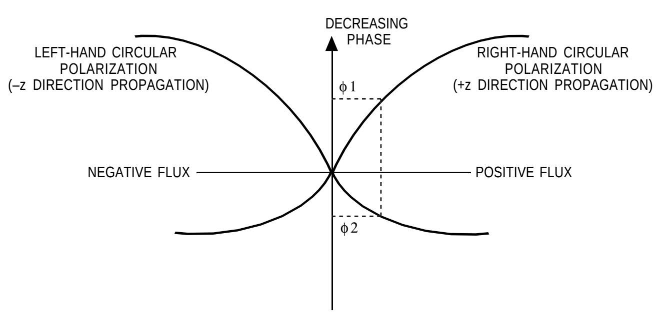

Fig. 2-3 Phase characteristics of I-30 phase shifter

III. Feed Design

The RF feed assembly is shown pictorially in Figure 3-1. The feed must efficiently illuminate the lens, provide monopulse operation on receive and provide transmitter-receiver duplexing. Prior art [1] has used four orthomode transducers (OMT) in a cruciform with input ports to each OMT fed in phase quadrature to obtain circular polarization. This results in a feed with a costly and complicated external waveguide network. The novelty of the new feed design is in the use of four septum polarizers in the cruciform for the generation of CP. As in prior designs, accommodation of high power is achieved through the factor of four reduction in the input transmitter power by use

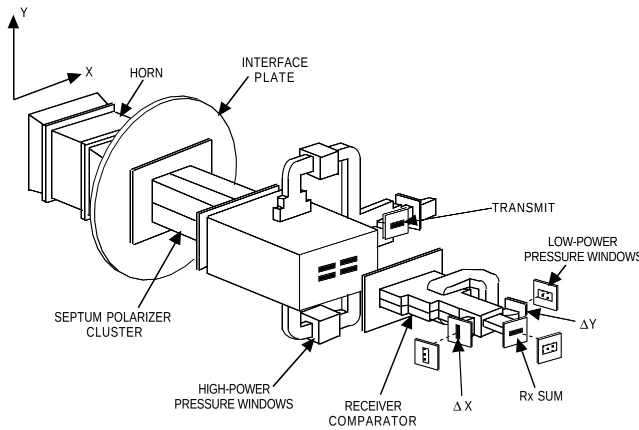

Fig. 3-1 RF feed assembly

of the cruciform. Physically the feed is pressurized, and the septum polarizer cluster is removable to allow for operation with the opposite sense circular polarization. A block diagram of the feed is shown in Figure 3-2.

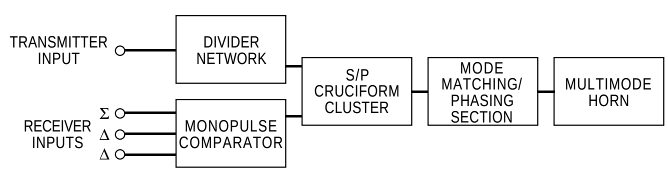

Fig. 3-2 Multimode feed block diagram

The waveguide network which combines the Tx ports of the septum polarizers to form a single transmitter input is connected as shown in Figure 3-3. Since the average input power is greater than the average power capacity of off-the-shelf pressure windows, the windows are inserted into the lines after the first Magic Tee. The power in each line is again divided into equal parts with folded H-plane tees and this results in four equiphase signals for excitation of the septum polarizer cluster on transmit.

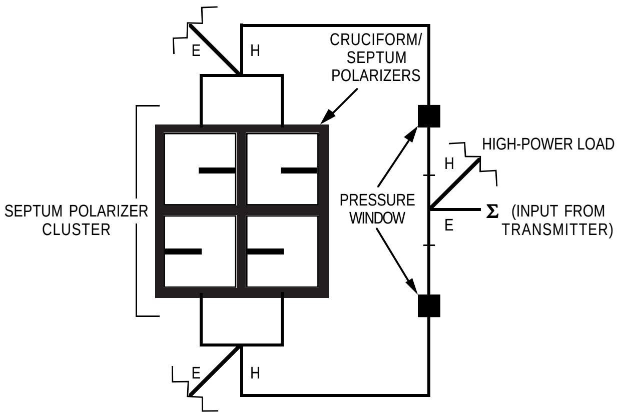

Fig. 3-3 Transmit network schematic

The septum polarizer is a four-port waveguide device, and the stepped septum version described by Chen and Tsandoulas [2] is shown in Figure 3-4. The square waveguide at one end constitutes two ports since it supports two orthogonal modes. The stepped septum divides the square waveguide into two rectangular waveguides sharing a common wall. If one of the rectangular waveguide ports is excited, the signal is transformed into a circularly polarized signal at the square waveguide. Exciting the other rectangular port results in the opposite sense of circular polarization at the square port.

The operation of the septum polarizer is also illustrated in Figure 3-4. Assume the square port is excited with an electric field parallel to the septum. This signal transforms into two odd-mode signals at the rectangular ports. An electric field perpendicular to the septum transforms into two even-mode signals as shown. If both input components exist simultaneously, cancellation at one or the other rectangular port occurs if the amplitudes are identical and the phase difference is either zero degrees or 180 degrees. Since the septum is designed to provide 90 degrees of differential phase shift, isolation occurs for circularly polarized input signals.

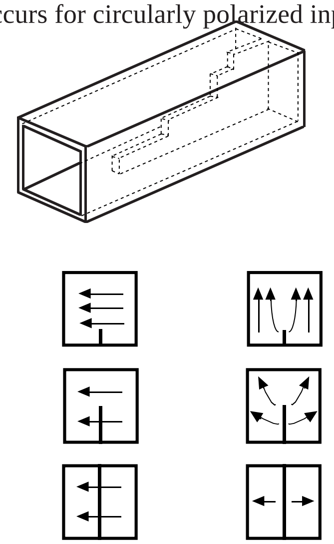

Fig. 3-4 Septum Polarizer

Monopulse operation on receive is accomplished by means of a standard monopulse comparator connected to the receive ports of the septum polarizer cluster. This is a commercially available off-the-shelf item and provides the excitations to the Rx ports of septum polarizers necessary to develop sum and difference patterns. The excitations and the resulting modes generated in the mode matching section are shown in Figure 3-5. Since this is a circularly polarized application, six different waveguide modes are launched at the cruciform section. The circularly polarized azimuth difference patterns are formed by the TE_{20} mode and the horizontally polarized hybrid TE/TM-11 mode phased 90 degrees in time, while the elevation difference pattern results from the vertically polarized TE/TM_{11} hybrid mode and the TE_{02} mode similarly phased. Since these modes have different phase velocities, a difference mode phasing section is used at the throat of the multi-mode horn to obtain the necessary time quadrature at the aperture of the feed horn.

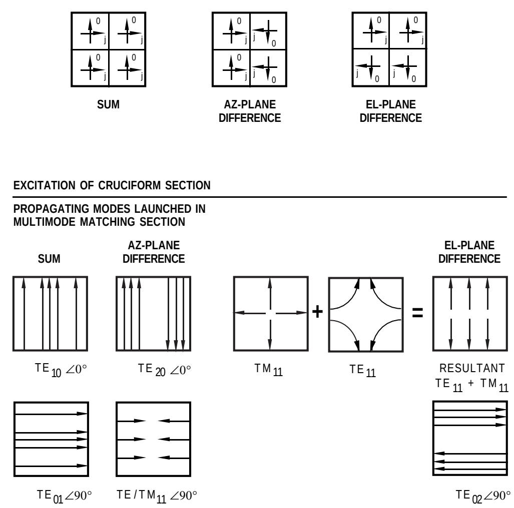

Fig. 3-5 Mode excitation of multimode feed by monopulse network

Efficient illumination of the phased lens requires that the feed horn patterns be rotationally symmetric with low sidelobes. This requires that the dominant TE_{10} uniform E-plane field distribution in the horn be altered to more nearly match that of the H-plane which possesses a cosine distribution. This is accomplished with a square multimode horn which uses flare angle changes[3] as the mechanism for generating higher order modes needed for control of the primary sum patterns. The horn geometry is shown in Figure 3-6 and as can be seen it simple and easy to fabricate. Rotationally symmetric patterns over 10 to 12 percent bandwidths can be obtained with this

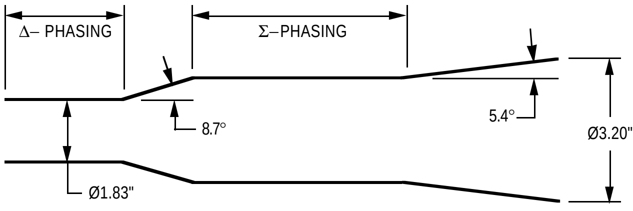

Fig. 3-6 Multi-flare multimode horn design

technique.

Figure 3-7 shows the modes involved in tapering the E-plane field distribution to nearly match that of the H-plane. Each flare angle change excites symmetric higher order modes with amplitude inversely related to the mode order and directly as the magnitude of the flare angle change. For equal E- and H- plane 10dB beamwidths, it is necessary that the amplitude of the TE/TM_{12} mode relative to the TE_{10} mode be about 0.66 in voltage. (A small amount of TE_{30} mode is also excited, but can be ignored for small flare angle changes.) This determines the magnitude of the flare angle. The length of the square straight section in conjunction with the overall horn length, is chosen so that the hybrid TE/TM_{12} mode arrives at the aperture of the horn in phase with the TE_{10} mode. Note that with circular polarization excitation the equivalent orthogonal waveguide modes are generated in time quadrature.

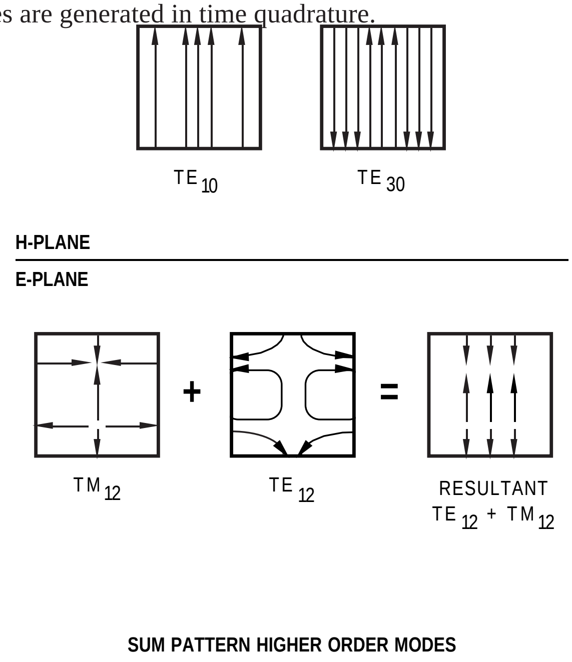

Fig. 3-7 Multimode horn pattern control

Typical CP sum patterns, measured on a near-field range for the horizontal (H) and elevation (E) planes, are shown in Figure 3-8. The cross-polarization level over the angle subtended by the lens (27 degrees) was measured in the range of -18 to -24dB corresponding to axial ratios of 2.1 to 1.1dB. Difference patterns for both planes are shown in Fig. 3-9. Note that E- and H-plane refer to elevation and horizontal plane respectively.

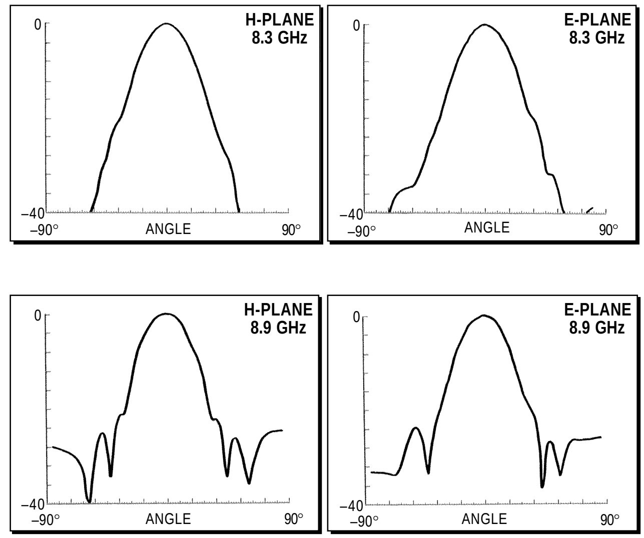

Fig. 3-8 RCP Feed Patterns Receive Sum

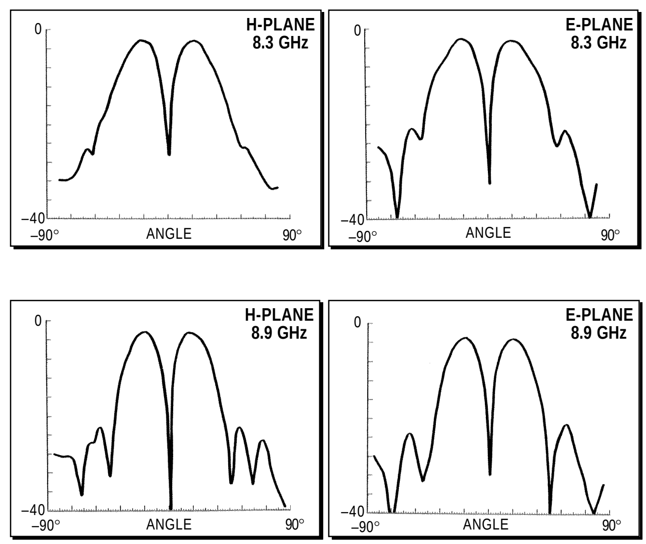

Fig. 3-9 RCP feed patterns difference

IV. Secondary Pattern and Gain Measurements

Extensive secondary pattern and gain characteristics were measured on a near-field antenna range. This facility was designed and built by MAG expressly for the secondary pattern measurements on this array. A seven foot by seven foot scanner, shown in Figure 4-1, was purchased and interfaced to an HP 200 series computer. Software was written for control of the scanner and data acquisition and control of the HP 8510B network analyzer which served as a receiver. The measurement probe is a septum polarizer with axial ratio less than 0.4 dB. Data was taken simultaneously for both senses of CP. The NIST Planar Nearfield Software package was used for transforming near-field data to the far field.

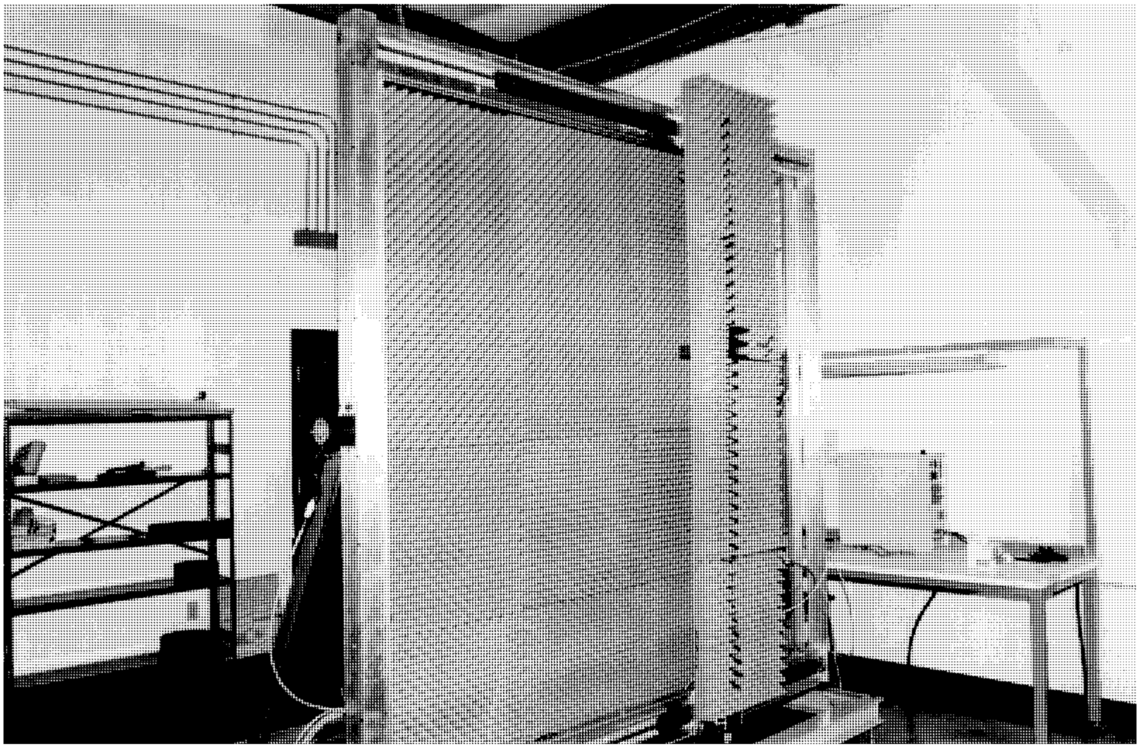

Fig. 4-1 Seven foot by seven foot scanner

Collimation of the array was also performed with the near-field scanner. The probe is positioned sequentially over each element in the array and its phase shifter commanded through all of its phase states while the others are at a fixed phase state. Referring to the diagram in Figure 4-2, the fixed phasor corresponding to the phase shifters not being cycled is subtracted from the measurement and a "best fit" circle is used to obtain the phase shifter command which aligns the element phasor to the fixed phasor. This procedure is iterated several times and no more than three passes through all of the elements are required for collimation. Figure 4-3 and Figure 4-4 shows measured near-field amplitude and phase data at center band transformed back to the aperture plane after three iterations of the collimation procedure.

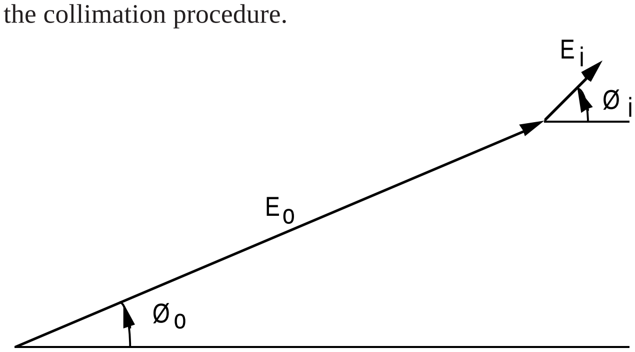

Fig. 4-2 Collimation procedure phasor diagram

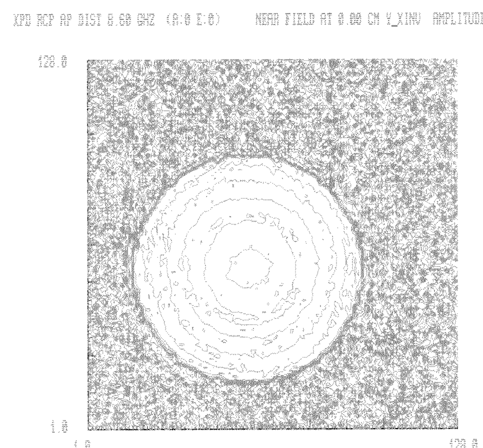

Fig. 4-3 Aperture plane amplitude (3dB contours)

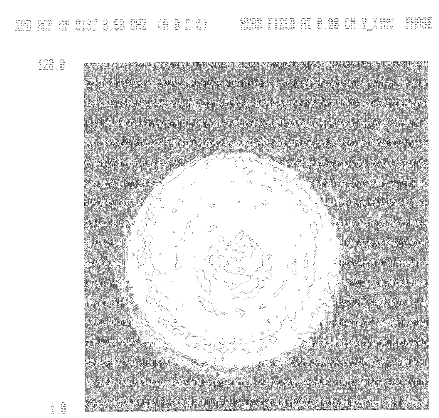

Fig. 4-4 Aperture plane phase (30 Degree contours)

Measurements were made for various beam scan angles, polarization and frequency on the receive sum and difference ports and the transmit sum port. Parameters measured included gain, beamwidth and sidelobe levels and are summarized in Table 4-1 for boresight scan. Note that the peak cross polarization in the secondary patterns is lower than that of the primary feed patterns. This arises from the fact that non-reciprocal phase shifters are used in the array. When, for example, the phase shifters are set to collimate a RHCP beam on transmit, LHCP energy resulting from the feed cross polarization is not collimated. Therefore, this energy is radiated over a wide range of spatial angles thereby yielding lower secondary cross polarization levels.

Table 4-1
Antenna Boresight Characteristics

			RHCP CLUSTER"		LHCP CLUSTER*	
Freq.	Beam Position	Parameter	Transmit Port	Receive Port	Transmit Port	Receive Port
8.3 GHz	Az:0/El:0	Gain	36.31	36.36	36.23	36.51
		AZ Beamwidth	1.97	1.98	1.96	1.96
		EL Beamwidth	1.98	1.98	1.98	1.97
		Cross Pol	-30.44	-26.4	-28.86	-26.22
		AZ Sidelobe	-27.44	-23.87	-26.03	.26.17
		EL Sidelobe	-30.06	-29.88	-29.28	-29.69
8.5 GHz	Az:0/El:0	Gain	36.08	35.94	35.83	36.26
		AZ Beamwidth	1.97	1.95	1.99	1.99
		EL Beamwidth	1.97	1.97	1.98	1.98
		Cross Pol	-26.06	-26.4	-24.32	-26.25
		AZ Sidelobe	-31.59	-24.80	-27.86	-27.75
		EL Sidelobe	-29.66	-29.19	-27.16	-26.34
8.9 GHz	Az:0/El:0	Gain	37.44	35.76	36.27	34.75
		AZ Beamwidth	1.87	1.95	1.86	1.87
		EL Beamwidth	1.88	1.91	1.85	1.84
		Cross Pol	-23.09	-24.07	-26.32	-26.19
		AZ Sidelobe	-19.94	-28.58	-21.72	-21.90
		EL Sidelobe	-25.43	-26.67	-21.33	-23.54

*REFERS TO SENSE OF CIRCULAR POLARIZATION TRANSMITTED BY ANTENNA

Representative co and cross-polarized RCP transmit sum patterns are shown in Figures 4-5 and 4-6 while the corresponding receive sum patterns (LCP) are shown in Figure 4-7 and Figure 4-8 for boresight and maximum scan condition. Figure 4-9 shows the co and cross-polarization LCP transmit patterns and and Figure 4-10 shows the receive sum patterns (RCP) for maximum scan.

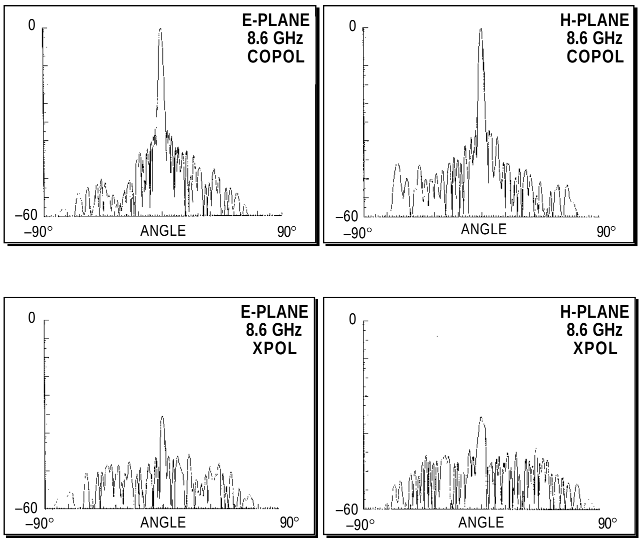

Fig. 4-5 Transmit RCP Patterns Boresight

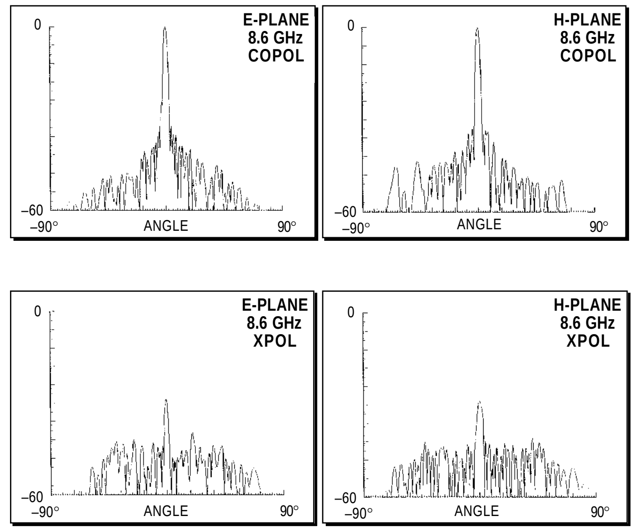

Fig. 4-7 Receive LCP patterns boresight

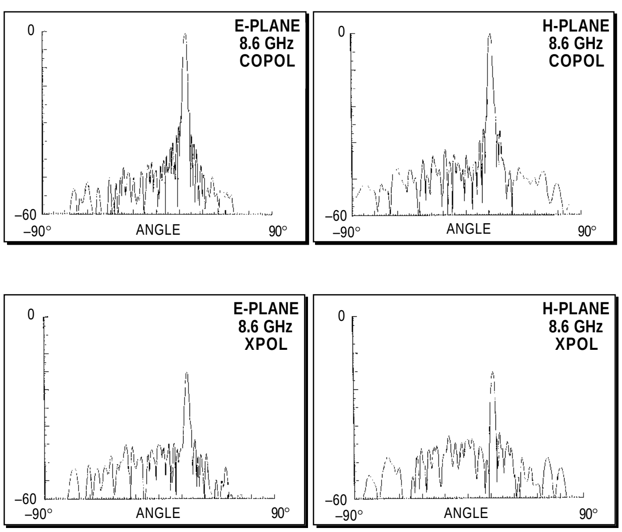

Fig. 4-6 Transmit RCP patterns maximum scan condition

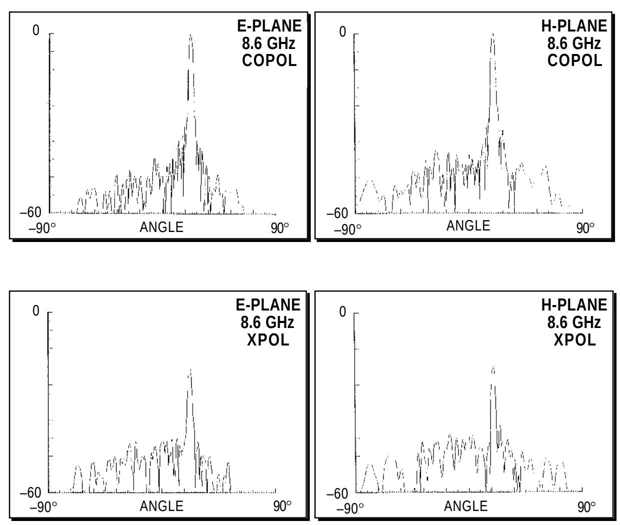

Fig. 4-8 Receive LCP patterns maximum scan condition

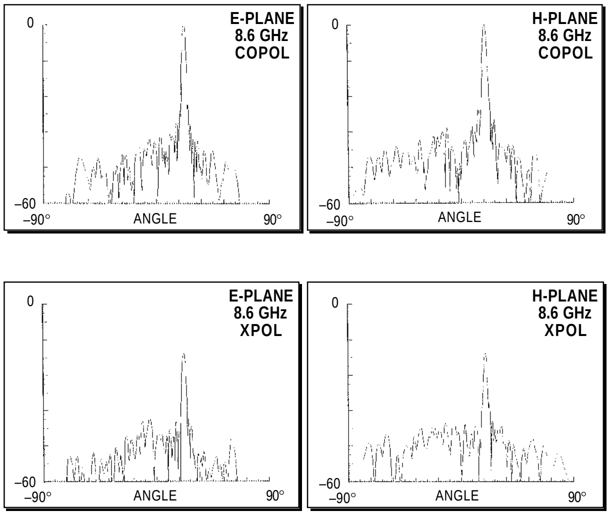

Fig. 4-9 Transmit LCP patterns maximum scan conditions

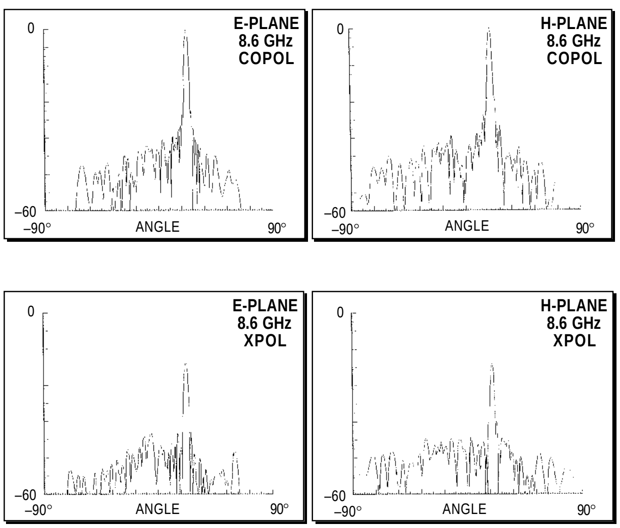

Fig. 4-10 Receive RCP patterns maximum scan condition

Typical difference patterns in the elevation and horizontal planes at boresight are shown in Figure 4-11. The low sidelobes exhibited by these patterns are inherent in space fed arrays using a monopulse multimode feed.

V. Conclusions

The results of this work indicate that an efficient circularly polarized feed capable of transmitting high power for a space fed phased array can be realized using four stepped septum polarizers in a cruciform arrangement. Use of a multimode multi-flare horn is shown to provide very good secondary pattern performance in both the transmit and monopulse modes of operation.

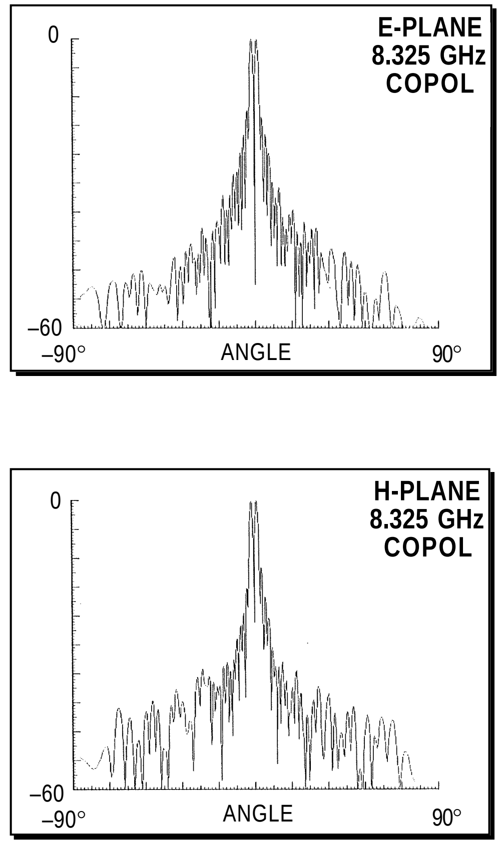

Fig. 4-11 Receive LCP difference patternsboresight

VI. Acknowledgements

This work was performed for the U.S. Naval Air Warfare Center, China Lake, CA under a subcontract from Loral Space & Range Systems, Ridgecrest, CA. The authors wish to acknowledge the support of NAWC, Loral and Microwave Applications Group.

VII. References

1. Goudey, K.R. and Sciambi, A.F. (1978) "High Power X-Band Monopulse Tracking Feed for the Lincoln Laboratory Long-Range Imaging Radar," IEEE Trans. on Microwave Theory and Techniques, Vol. MTT-26, No. 5, May 1978, pp. 326-332.

2. Chen, M.H. and Tsandoulas, G.N. (1973) "A Wide-Band Square Waveguide Array Polarizer," IEEE Trans. on Antennas and Propagation, Vol. AP-21, No. 3, pp. 389-391.

3. Cohn, S.B., (1970) "Flare-Angle Changes in a Horn as a Means of Pattern Control," Microwave Journal, Vol. 13, No. 10, Oct. 1970, pp. 41-ff.